U–Pb detrital zircon analysis of the lower allochthon of NW Iberia: age constraints, provenance and links with the Variscan mobile belt and Gondwanan cratons

RUBÉN DÍEZ FERNÁNDEZ[1*], JOSÉ R. MARTÍNEZ CATALÁN[1], RICARDO ARENAS[2], JACOBO ABATI[2], AXEL GERDES[3,4] & JAVIER FERNÁNDEZ-SUÁREZ[2]

[1]*Departamento de Geología, Universidad de Salamanca, 37008 Salamanca, Spain*

[2]*Departamento de Petrología y Geoquímica and Instituto de Geología Económica, Universidad Complutense/Consejo Superior de Investigaciones Científicas, 28040 Madrid, Spain*

[3]*Institut für Geowissenschaften, Mineralogie, Goethe-Universität, D-60438 Frankfurt am Main, Germany*

[4]*Department of Earth Sciences, Stellenbosch University, Private Bag X1, Matieland 7602, South Africa*

Abstract: Detrital U–Pb laser ablation inductively coupled plasma mass spectrometry zircon ages from six siliciclastic samples from the lower allochthon of NW Iberia are analysed to constrain their maximum sedimentation age and provenance, and to evaluate the connections to the adjacent tectonostratigraphic domains. Deposited in the external sections of the Gondwana platform, their maximum depositional age is latest Neoproterozoic (*c.* 560 Ma). Comparison of the age populations of the lower allochthon with those of the rest of the allochthonous and autochthonous units of NW Iberia suggests that the terranes located in the footwall of the Variscan suture should not be considered as exotic elements, but as contiguous pieces of the same continental margin transported onto the adjacent Gondwana mainland in Variscan times. The data are in agreement with the regional trend defined by the drop in Early Neoproterozoic and Mesoproterozoic zircon content upward in the tectonic pile, which had been previously proposed as a marker of proximity to the eastern part of the West African Craton. Based on the age spectra, the palaeoposition for the time of sedimentation is placed in northern Africa, between the West African and Saharan cratons. Particular attention is paid to the occurrence of an Early Neoproterozoic input, probably derived from the Pan-African Hoggar suture.

Determining the age and provenance of sedimentary rocks provides hints to place the processes that affected the Earth's crust in time and space. Access to such information in mobile belts surrounding stable cratons is limited by the fact that these belts usually are involved in active plate boundaries, where both deformation and metamorphism blur some of the age (fossils) and palaeogeographical (palaeomagnetism) indicators. Zircon is a common constituent of most sedimentary rocks, and it is very resistant and largely survives metamorphism and deformation. Therefore, the analysis of age populations of detrital zircon grains is commonly used to constrain the maximum depositional age and provenance of metasedimentary rocks, and its role as a geodynamic tracer is currently gaining importance (e.g. Braid *et al.* 2011; Drost *et al.* 2011; Zhu *et al.* 2011).

Sedimentary basins located around cratonic areas may be filled with detritus derived from the craton itself and/or from dismantlement of younger belts bounding the craton. Given that these belts typically contain a significant cratonic input, the origin of detritus after several recycling events is difficult to interpret by conventional, single zircon grain core provenance analyses. These analyses provide information about only one tectonomagmatic cycle. However, core and rim analyses offer a wider picture of the orogenic cycles recorded in the source areas because they not only can date the events, but also can reveal the age of the material involved in each cycle. Supported by a regional background, such data constrain the possible sources, improving the precision of the palaeogeographical reconstructions.

Formed from the Late Palaeozoic collision between Gondwana and Laurussia, the Variscan belt may be divided into three major domains: the external thrust belt and foredeep basin, the autochthonous sequences of Gondwana, and the allochthonous, far-travelled terranes, which show different derivation and include ophiolites (Fig. 1a; Martínez Catalán *et al.* 1997). The allochthon consists of rootless thrust stacks structurally emplaced on the autochthonous Gondwanan margin. In NW Iberia, the Schistose Domain is located at the base of the far-travelled terranes and is interpreted to represent a parautochthonous slice of the outer Gondwanan margin that was transported inland during the Variscan collision (Ribeiro *et al.* 1990; Martínez Catalán *et al.* 1997). Both the upper and lower limits of the Schistose Domain are tectonic contacts, either low-angle thrusts or extensional detachments, or both (González Clavijo & Martínez Catalán 2002; Martínez Catalán *et al.* 2002; Díez Montes *et al.* 2010; Gómez Barreiro *et al.* 2010; Díez Fernández *et al.* 2012*b*), which obscure former tectonic boundaries as well as the links of the lower allochthon with the adjacent terranes; namely, the autochthon, and other allochthonous units.

The Variscan nappes may represent the amalgamation of terranes that were previously contiguous along the northern margin of Gondwana (Martínez Catalán 1990; Gómez Barreiro *et al.* 2007). To determine the maximum depositional age and constrain the provenance, here we present laser ablation inductively coupled plasma mass spectrometry (LA-ICP-MS) U–Pb ages of detrital zircons from six siliciclastic samples of the lower allochthon of NW Iberia (Schistose Domain). To date, such analysis has not been

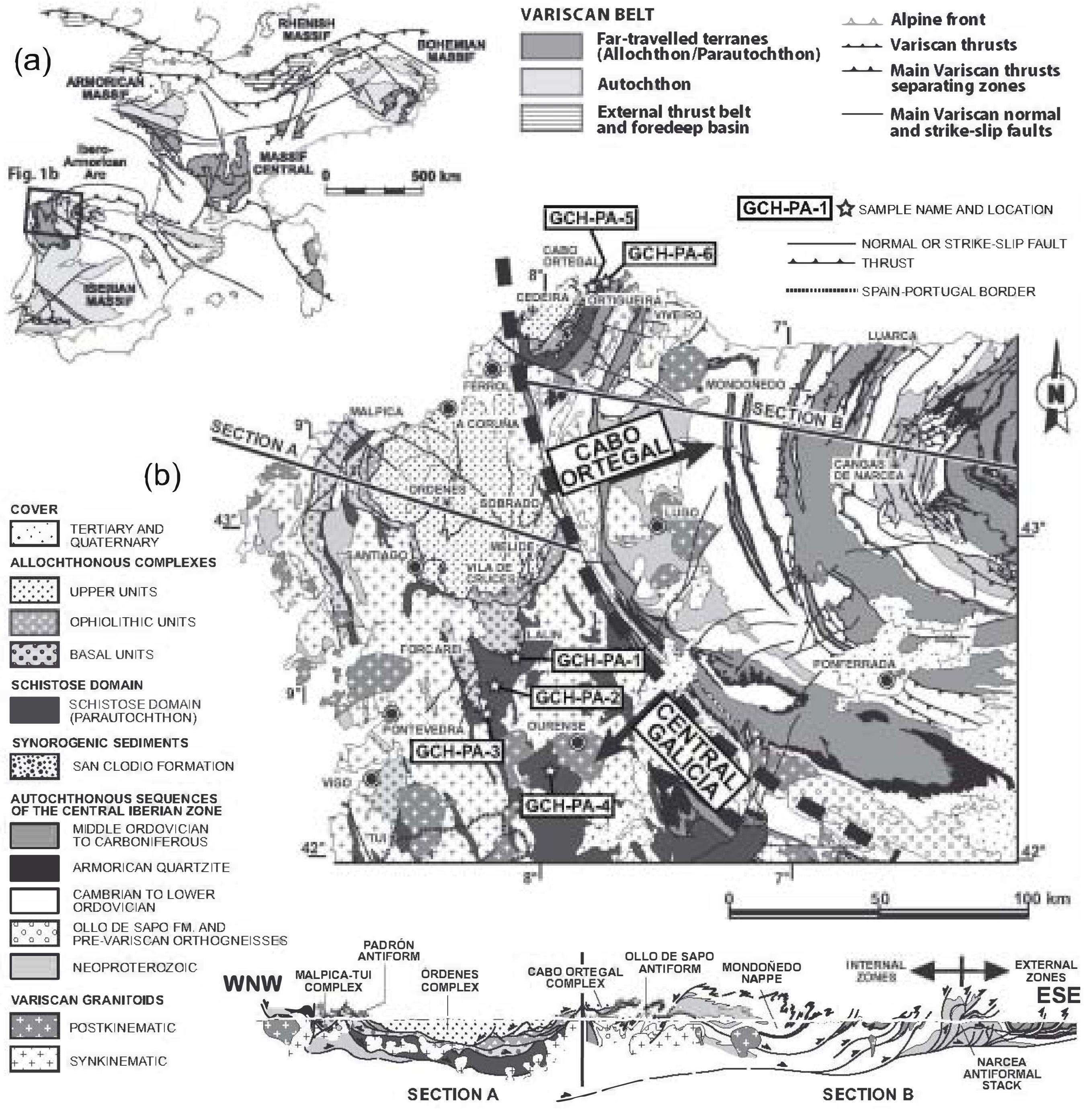

Fig. 1. (**a**) Location of the study area in the Variscan belt. (**b**) Map and representative cross-section of the NW Iberian Massif showing the general structure. The location of the samples analysed is included. The bold dashed line separates the two main regions of Galicia (Spain) in which the Schistose Domain crops out.

performed either in this domain or in other equivalent sections along the Variscan belt. The cratonic affinities of this domain are then compared with those of the overlying and underlying terranes of the tectonic pile to determine their relative palaeogeographical positions during sedimentation and to evaluate the internal homogeneity of the allochthonous nappe stack of NW Iberia in terms of age populations and provenance. In addition, a core–rim analysis conducted on zircon grains showing multiple stages of crystallization is used to reveal the crustal recycling events that affected the source areas, thereby providing further constraints for palaeogeographical reconstructions.

Geological setting

The Variscan allochthonous terranes of NW Iberia crop out as klippen in synformal structures (Fig. 1b; Martínez Catalán *et al.* 2009). The upper part of the nappe stack crops out in the allochthonous complexes, which include several types of tectonometamorphic units (Arenas *et al.* 1986). The upper units are tectonic slices of a Cambro-Ordovician continental arc built on the Gondwana margin (Abati *et al.* 1999; Fuenlabrada *et al.* 2010), whereas the middle units are ophiolitic and considered relicts of oceanic domains flanking the Gondwanan platform (Díaz García *et al.* 1999; Pin *et al.* 2006; Arenas *et al.* 2007; Sánchez Martínez *et al.* 2007). The basal units represent the most external part of the Gondwana margin (Arenas *et al.* 1995; Martínez Catalán *et al.* 1996) and preserve evidence of the continental rifting and tectonomagmatic activity connected to both the building of the Cambro-Ordovician arc system and the opening of an ocean basin (Díez Fernández & Martínez Catalán 2009; Abati *et al.* 2010; Díez Fernández *et al.* 2012*a*).

The lower part of the allochthonous stack forms an imbricate thrust sheet known as the Parautochthon (Ribeiro *et al.* 1990) or Schistose Domain (Marquínez García 1984), which separates the far-travelled terranes from the autochthonous sequences of Gondwana. The base of the Schistose Domain is a low-angle thrust that cuts earlier folds toward the foreland (Farias *et al.* 1987; Marcos & Farias 1999; Díez Montes *et al.* 2010). The domain itself is characterized by a widespread, flat-lying foliation and low- to medium-grade metamorphism at the top (Barrovian-type evolution) and partial melting conditions at the bottom. The upper parts of allochthonous nappe stack preserve the record of the early Variscan crustal thickening related to folding and thrusting during initial convergence, whereas the lower parts are intruded by extensive Variscan granitoids (Fig. 1b) and were reworked in migmatitic domes that developed during the extensional collapse of the orogenic belt (e.g. Díez Fernández *et al.* 2012*b*).

From a stratigraphic point of view, the Parautochthon or Schistose Domain, which forms the lower parts of the nappe stack, consists of preorogenic Cambrian, Ordovician, Silurian and Devonian metasedimentary and metavolcanic rock sequences, and younger, Late Devonian and Early Carboniferous synorogenic flysch deposits (Iglesias & Robardet 1980; Pereira *et al.* 1999; Sarmiento *et al.* 1999; Gutiérrez-Marco *et al.* 2001; González Clavijo & Martínez Catalán 2002; Farias & Marcos 2004; Rodríguez *et al.* 2004; Valverde-Vaquero *et al.* 2005; Piçarra *et al.* 2006). The stratigraphic, magmatic and faunal similarities between this domain and the Iberian autochthonous sequences (Farias *et al.* 1987; Barrera *et al.* 1989; Valverde-Vaquero *et al.* 2005; Piçarra *et al.* 2006), together with the absence of ophiolites inside or at their contact, suggest that the two domains were located adjacent to each other, forming part of the same continental margin.

Sample description

The samples were collected in the low- to medium-grade sections of the Schistose Domain (Fig. 1b). In central Galicia, the Schistose Domain is up to 7 km thick and may be divided in three lithostratigraphic units (Barrera *et al.* 1989; Farias & Marcos 2004). There, its lower part is known as the Santabaia Group, which is a volcano-sedimentary series including quartz and mica schists, paragneisses, felsic metavolcanic rocks, and minor layers of calc-silicate, amphibolite, quartzite, and mica-rich quartzite. In an intermediate position, the Nogueira Group consists of black to greyish mica schists, carbonaceous chert layers (lydite), quartz schists and lenses of calc-silicate and marble, whereas in the uppermost position the Paraño Group is mostly composed of quartz schists (samples GCH-PA-1, 2, and 3) and phyllites, together with layers of metagreywacke, quartzite (sample GCH-PA-4) and felsic metavolcanic rocks (Marquínez García 1984; Gallastegui *et al.* 1987; Marcos & Llana-Fúnez 2002). Around the Cabo Ortegal Complex, the Schistose Domain is up to 3 km thick, and is divided from bottom to top into the Loiba and Queiroga Series (Marcos & Farias 1999). The Loiba Series consists of phyllites (sample GCH-PA-6) alternating with minor layers of grey to white quartzite, felsic metavolcanic rocks and metavolcano-sedimentary rocks. The Queiroga Series includes thin-bedded grey feldspathic lithic metasandstone alternating with phyllite, quartzite (sample GCH-PA-5) and metavolcanic rocks (Ancochea *et al.* 1988; Arenas 1988).

The metasedimentary rocks of the Schistose Domain represent a rather azoic series, therefore we lack good age constraints for the samples collected. The age of the Santabaia Group has been assumed to be Precambrian–Silurian (Barrera *et al.* 1989), but recent U–Pb ages from two volcanic complexes in an equivalent succession in Trás-os-Montes (NE Portugal) have yielded Late Cambrian and Early Ordovician ages in the lower and middle parts of the sequence respectively (Dias da Silva *et al.* 2012). The Nogueira and Paraño groups are considered to be of Silurian and Silurian–Devonian age, respectively (Marquínez García 1984; Barrera *et al.* 1989). For the sequences of Cabo Ortegal, previous studies have confirmed an Ordovician age in the upper part of the Loiba Series (Llanvirn–Caradoc Chitinozoa; Rodríguez *et al.* 2004) and in the upper part of the Queiroga Series (metavolcanic rocks of *c.* 475 ± 2 Ma; Valverde-Vaquero *et al.* 2005).

GCH-PA-1 (UTM 572622 E, 4717334 N) is a mylonitic quartzite of the Paraño Group sampled to the south of Lalín (Silurian–Devonian age), adjacent to the basal thrust of the Lalín and Forcarei units (Fig. 1b). It consists of quartz, biotite and white mica, with minor feldspar, mainly plagioclase, chlorite and opaque minerals. The mylonitic foliation is defined by narrow strips of mica separating bands of recrystallized quartz grains showing triple junctions, and in many cases, rectangular shapes. The larger grains commonly include small mica grains oriented parallel to the foliation, indicating that mylonitization gave rise to a fine-grained fabric that evolved to a coarse-grained fabric as a result of temperature increase at the end of or after thrusting. The latter is proved by almandine and staurolite growth overprinting the foliation of adjacent mica schists. Chlorite appears as a late, retrograde phase, mostly replacing parts of the mica-rich layers.

GCH-PA-2 (UTM 563693 E, 4705273 N) is a micaceous quartzite of the Paraño Group collected farther to the SW in the late Variscan antiform between the Forcarei and Lalín units (Silurian–Devonian age). It is similar in composition to the previous sample, except for the absence of plagioclase, and has a strongly developed, non-mylonitic schistosity. Quartz grains are clearly deformed but less recrystallized, usually elongated but irregular in shape, with small-amplitude lobate contacts and common but not dominant triple junctions. Crossed micas and poorly preserved hinges in the quartz-rich domains provide evidence of a previous tectonic foliation, overprinted by the dominant main schistosity, which is related to the emplacement of the allochthonous complexes above (Marquínez García 1984).

GCH-PA-3 (UTM 561396 E, 4698080 N) is a biotite-rich schist collected in the Paraño Group (Silurian–Devonian age), close to the southern part of the Forcarei Unit and the Lalín–Forcarei thrust. It has a well-developed tectonic foliation with irregularly distributed quartz-rich domains suggesting that it was derived from a tectonic banding developed from crenulation of a previous cleavage. Sets of oblique, large grains and recrystallized fold hinges in mica-rich domains confirm that we are dealing with an evolved crenulation cleavage. The size of the mica grains involved indicates that the previous foliation was a coarse-grained schistosity, probably the second, regionally developed foliation related to the emplacement of the allochthonous complexes. This relatively old foliation was thermally overprinted during the metamorphic peak, and then underwent microfolding contemporaneous with the development of the late Variscan steep folds affecting the allochthon and

Schistose Domain. Growth of chlorite sheaves cross-cutting the foliation characterizes late-stage retrogradation.

GCH-PA-4 (UTM 584005 E, 4680268 N) is a quartzite sampled to the south of Ourense, in the open structural basin of A Seara, and represents the uppermost preserved parts of the Paraño Group (Silurian–Devonian age). It is a low-grade, strongly deformed rock characterized by large quartz porphyroclasts with irregular, serrate boundaries, undulose extinction, and recovery process, floating in a matrix of finely recrystallized quartz grains. Micas, almost exclusively chlorite, occur in irregular bands with widths that vary along strike. Oxides bounding the strips, mainly their narrow parts, indicate pressure solution mechanisms in the formation of the foliation, whereas the quartz fabrics suggest recrystallization by subgrain rotation.

GCH-PA-5 (UTM 596882 E, 4841674 N) is a quartzite sampled in the upper part of the Queiroga Series, close to the base of the Cabo Ortegal Complex (Ordovician age). The rock is moderately deformed, with most grains elongated and showing a preferred orientation, but their elongation is weak in general, with aspect ratios of 1–2. Grain boundaries are serrate, and undulose extinction is always present. Tiny white micas separate some of the quartz grains and, together with the elongated quartz grains, delineate the only identifiable tectonic fabric, which clearly developed under low-temperature conditions.

GCH-PA-6 (UTM 600970 E, 4844545 N) is a finely laminated, fine-grained, low-grade metapelite formed by quartz, white mica, and opaque minerals. It was collected at the lower part of the Loiba Series, close to the basal thrust of the Schistose Domain to the east of the Cabo Ortegal Complex. A cleavage that is only slightly oblique to the sedimentary banding can be seen in the thin section, although in outcrop it can be seen also cutting at high angles the primary layering and probably a low-grade cleavage subparallel to it.

Analytical methods: U–Pb zircon dating

Zircon grains were recovered at Universidad Complutense, Madrid by crushing, sieving and concentration of the heavy fraction using a Wilfley table, followed by magnetic and density separation. The final mineral fractions were hand-picked under a binocular microscope, mounted in epoxy resin, and then polished to an equatorial section of the grains at Goethe-University, Frankfurt.

All samples contain subidiomorphic zircons with rounded rims and variable shape and size. Their colour varies from clear and colourless to pinkish and almost opaque. The internal structure, inclusions, fractures and physical defects were analysed using cathodoluminescence (CL) imagery at Goethe-University, Frankfurt. The CL study shows that most zircon grains have a similar core–rim internal texture. The cores usually exhibit concentric oscillatory zoning, suggesting crystallization in granitic magmas (Hoskin 2000). Only the most homogeneous parts of the grain cores, free of defects, cracks and inclusions, were analysed. Some grains exhibit multiple and concentric layers of growth, which were analysed when possible.

Uranium and lead isotopes were analysed using a ThermoScientific Element 2 sector field ICP-MS system coupled to a New Wave Research UP-213 ultraviolet laser system at Goethe-University, Frankfurt following the method of Gerdes & Zeh (2006).

The data were acquired in time-resolved–peak jumping–pulse counting mode over 670 mass scans during 19 s background measurement followed by 25 s sample ablation. Laser spot sizes varied from 20 to 30 µm with a typical penetration depth of *c.* 15–20 µm. The signal was tuned for maximum sensitivity for Pb and U while keeping oxide production, monitored as $^{254}UO/^{238}U$, well below 1%. A teardrop-shaped, low-volume (<2.5 cm^3) laser cell with fast response (<1 s) and low wash-out time was used (Janousek *et al.* 2006; Frei & Gerdes 2009). With a depth penetration of *c.* 0.6 µm s^{-1} and a 0.9 s integration time (=15 mass scans=1 ratio) any significant variation of the Pb/Pb and U/Pb at the micrometre scale is detectable.

Raw data were corrected offline for background signal, common Pb, laser-induced elemental fractionation, instrumental mass discrimination, and time-dependent elemental fractionation of Pb/U using an in-house MS Excel® spreadsheet program (Gerdes & Zeh 2006, 2009). A common Pb correction based on the interference- and background-corrected ^{204}Pb signal and a model Pb composition (Stacey & Kramers 1975) was carried out, where necessary. The necessity of the correction was based on whether or not the corrected $^{207}Pb/^{206}Pb$ lay outside the internal errors of the measured ratios.

Uncertainties related to the common Pb correction (e.g. 4% uncertainty on the assumed $^{207}Pb/^{206}Pb$ composition) were quadratically added to final uncertainty. The interference of ^{204}Hg (mean=129±18 c.p.s.) on mass 204 was estimated using a $^{204}Hg/^{202}Hg$ ratio of 0.2299 and the measured ^{202}Hg. Laser-induced elemental fractionation and instrumental mass discrimination were corrected by normalization to the reference zircon GJ-1 (Jackson *et al.* 2004). Prior to this normalization, the drift in inter-elemental fractionation (Pb/U) during 25 s sample ablation was corrected for single analyses. The correction was made by applying a linear regression through all measured ratios, excluding the outliers (±2 standard deviation; 2SD), and using the intercept with the y-axis as the initial ratio. The total offset of the measured drift-corrected $^{206}Pb/^{238}U$ ratio from the 'true' isotope dilution thermal ionization mass spectrometry (ID-TIMS) value of the analysed GJ-1 grain was typically around 3–9%. Reported uncertainties (2σ) of $^{206}Pb/^{238}U$ were propagated by quadratic addition of the external reproducibility (2SD) obtained from the standard zircon GJ-1 (n=12; 2SD *c.* 1.3%) during the analytical sequence (55 unknowns plus 12 GJ-1) and the within-run precision of each analysis (2 SE; standard error).

The external reproducibility of the $^{207}Pb/^{206}Pb$ of GJ-1 was about 0.9% (2SD). However, as $^{207}Pb/^{206}Pb$ uncertainty during LA-SF-ICP-MS analysis is directly dependent on ^{207}Pb signal strength, uncertainties were propagated following Gerdes & Zeh (2009). The ^{235}U value was calculated from the ^{238}U value divided by 137.88 and the $^{207}Pb/^{235}U$ uncertainty by quadratic addition of the $^{206}Pb/^{238}U$ and the $^{207}Pb/^{206}Pb$ uncertainty. Repeated analyses of reference zircon Plešovice yielded a concordia ages of 337.9±2.3 Ma (n=12), which is in agreement with the published value of 337.13±0.37 Ma (Sláma *et al.* 2008). The software ISOPLOT (Ludwig 2003) and AGEDISPLAY (Sircombe 2004) were used for plotting of the data and age calculation.

Age spectra

Only concordant or nearly concordant (<10% discordant) isotopic data were considered for interpretation of detrital zircon age. Figure 2 shows all the U–Pb concordia diagrams resulting from LA-ICP-MS analyses, and the probability and frequency diagrams are plotted in Figure 3. Ages younger than 1 Ga are reported based on $^{206}Pb/^{238}U$ ratios corrected for common Pb. Older ages are reported based on their ^{204}Pb-corrected $^{207}Pb/^{206}Pb$ isotopic ratio (e.g. Chang *et al.* 2006).

The most relevant features of the samples are summarized in Figure 4. Because no major differences between age groups of the six samples from the Schistose Domain have been found, their representative age populations are summarized in a cumulative probability diagram made by merging the data from all the samples (Fig. 5a). The main age group has Neoproterozoic $^{206}Pb/^{238}U$ ages

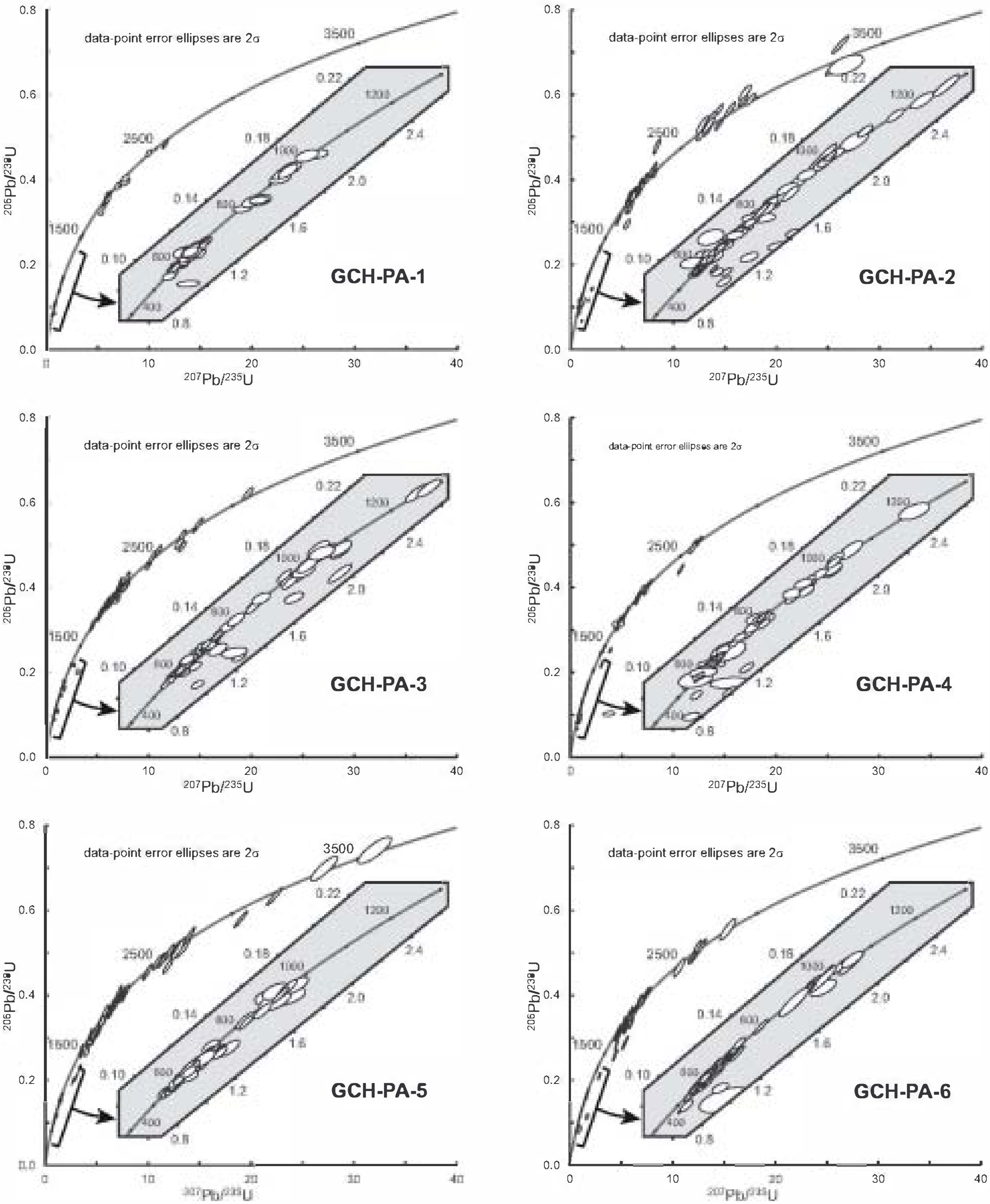

Fig. 2. U–Pb concordia diagrams showing the results of LA-ICP-MS analyses. Error ellipses represent 2σ uncertainties. Phanerozoic to late Mesoproterozoic ages have been enlarged for clarity.

between 550 and 750 Ma, with a maximum at 635 Ma. The second group includes analyses with Palaeoproterozoic $^{207}Pb/^{206}Pb$ ages between 1800 and 2250 Ma, showing three consecutive maxima at 1950, 2080, and 2150 Ma. There is a third group of Neo- to Mesoproterozoic ages straddling the interval between 750 and 1050 Ma, with relative maxima at 800, 950, and 1025 Ma. Some

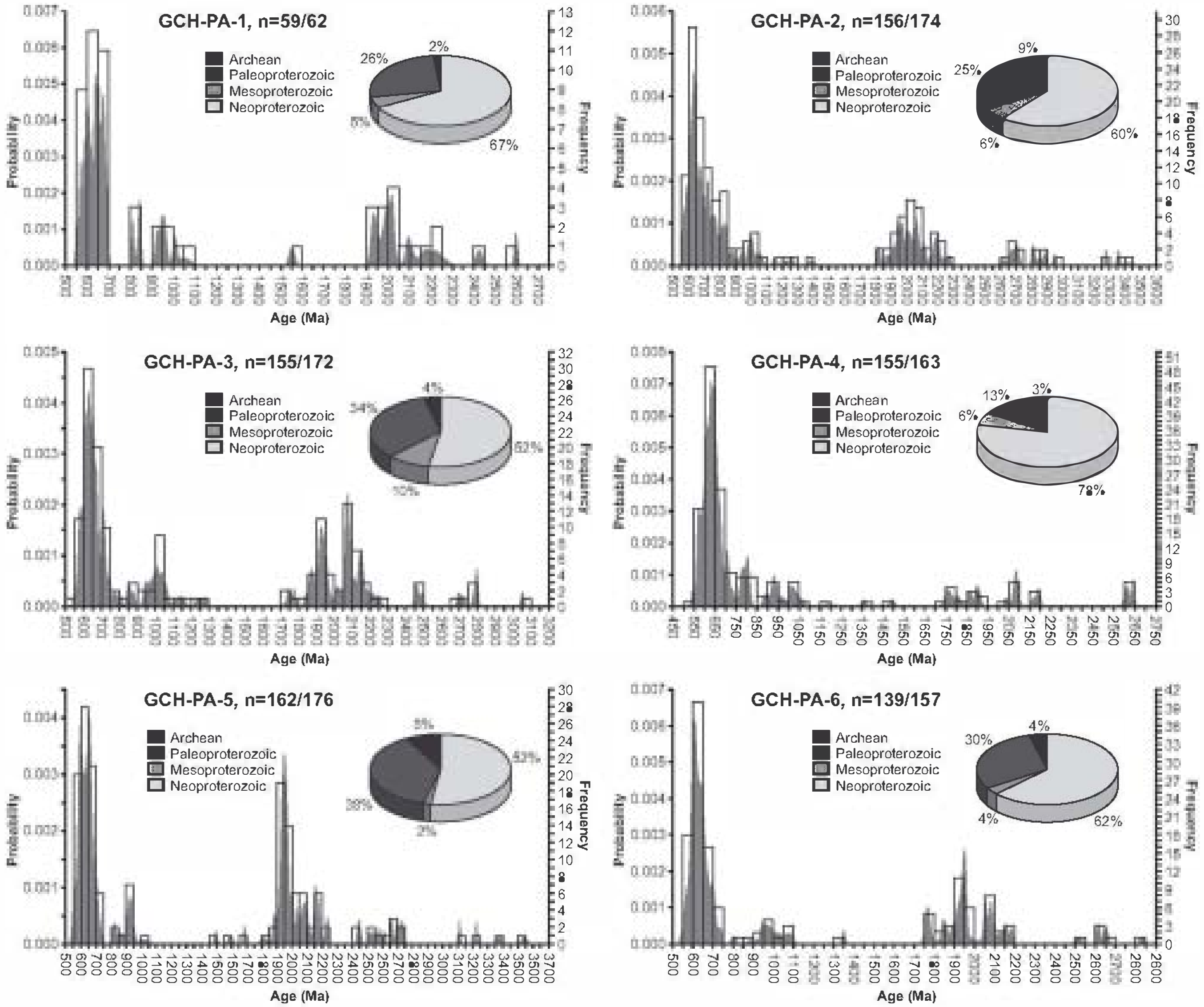

Fig. 3. Frequency (bars) and probability density distribution (curves) of U–Pb ages, and relative abundance of significant age populations (pie charts) of detrital zircon grains. *n*, number of analyses with <10% discordance/total number of analysed grains.

Archaean ages (mostly 2450–2800 Ma) plus a few small clusters ranging from 1050 to 1800 Ma complete the picture.

Among 74 core and rim analyses, 29 zircon grains from all samples except GCH-PA-4 yielded clearly different, concordant crystallization ages for their core and rim (Figs 6 and 7). The data provide evidence for crust recycling processes during the Palaeoproterozoic and Neoproterozoic. Recycling during the Palaeoproterozoic affected both the Archaean and Palaeoproterozoic grains, which were also involved in Mesoproterozoic and Neoproterozoic events. The Mesoproterozoic input participated in Early Neoproterozoic crust recycling, which extended to the Late Neoproterozoic and might have affected all the older age populations, including the Early Neoproterozoic input.

Discussion: depositional age, regional affinities, and palaeogeographical constraints

Based on both the youngest zircon grains and the youngest zircon age populations, the maximum age of sedimentation of all the samples is 560–550 Ma (Fig. 4). Faunal and isotopic dating, and correlation based on stratigraphical similarities indicate a Palaeozoic age (Cambrian, Ordovician, Silurian and Devonian) for the sequences of the Schistose Domain (see references above), although a Late Neoproterozoic age cannot be discarded for some of them, as no age indicators extend throughout the sedimentary record, and the fold and thrust structure of this domain is not well constrained (e.g. Valverde-Vaquero *et al.* 2005; Rodrigues *et al.* 2006; Dias da Silva & González Clavijo 2010).

In previous studies a marked scarcity of Early Palaeozoic zircon grains in the sedimentary record of the northern Gondwana platform has been noted (Fernández-Suárez *et al.* 2000, 2002; Martínez Catalán *et al.* 2004). Other researchers, however, have demonstrated that there was plenty of such input in the most external parts of the platform (Arenas *et al.* 2009; Díez Fernández *et al.* 2010). These data can be understood in the light of the major events characterizing the Early Palaeozoic evolution of this realm. The Early Palaeozoic input (mostly Cambrian) could have been supplied by the coeval peri-Gondwanan volcanic arcs (e.g. Abati *et al.* 1999;

	GCH-PA-1	GCH-PA-2	GCH-PA-3	GCH-PA-4	GCH-PA-5	GCH-PA-6
Main Age Group	550-700 (650)	560-850 (635)	550-700 (630)	545-700 (630)	550-700 (600-650)	550-700 (610)
Second Age Group	1920-2250 (1930, 2020)	1820-2270 (1950, 2050, 2200)	1850-2250 (1930, 2070, 2150)		1900-2200 (1950)	1750-2200 (1950)
Third Age Group	800-1050	850-1150	750-1250 (1000)		800-1050	800-1100
Youngest Zircon	553±13 (92%)	561±11 (97%)	549±14 (102%)	543±11 (109%)	551±19 (101%)	552±30 (95%)
Youngest Age Population	569	572	581	575	597	609
Oldest Zircon	2596±14 (98%)	3418±66 (97%)	3053±16 (102%)	2643±11 (100%)	3538±35 (101%)	2833±30 (100%)

Fig. 4. Table showing the most relevant features of the detrital zircon input of samples GCH-PA-1 to GCH-PA-6 (ages in Ma). Age sub-maxima are given in parentheses. Percentages indicate concordance.

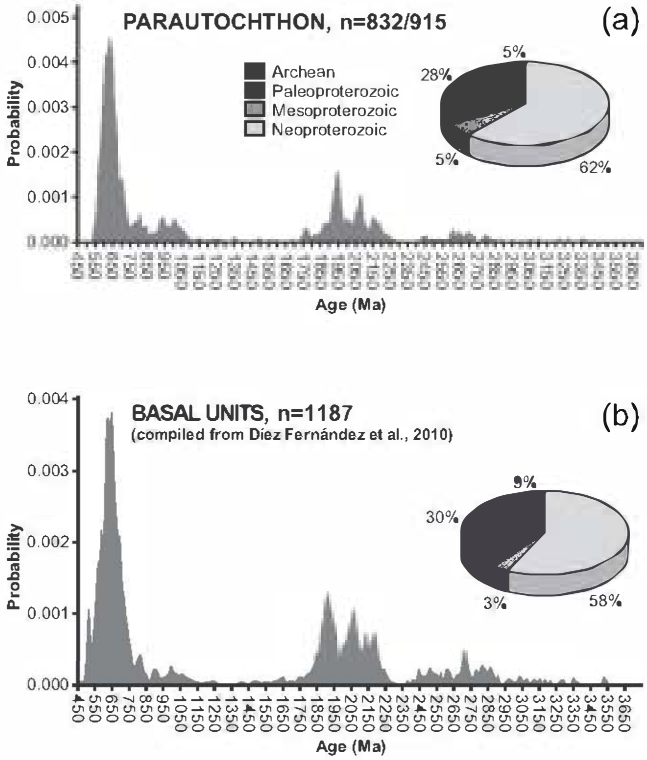

FIG. 5. Probability density distribution of U–Pb ages and relative abundance of significant age populations (pie chart) of detrital zircon grains from (a) the Schistose Domain (produced by merging the data from the six samples shown in Fig. 3) and (b) the basal units of the allochthonous complexes (compiled from Díez Fernández *et al.* 2010).

GCH-PA-1	2596±14	2427±30	2216±51	984±69
	2113±19	596±10	2022±15	642±13
	963±19	944±19	812±10	
	677±10	680±15	689±13	
GCH-PA-2	2820±17	2271±20	2196±32	2047±34
	633±17	809±21	1895±31	676±14
	1057±28	939±16	845±20	825±14
	726±12	834±17	661±32	646±19
	781±18	708±17		
	595±33	627±18		
GCH-PA-3	3053±16	2141±38	1274±28	668±18
	680±13	2015±20	940±21	612±14
GCH-PA-5	1944±46			
	722±25			
GCH-PA-6	2053±12	1933±23	1924±29	1909±17
	1948±14	1083±28	629±19	610±19
	1888±12	964±26	945±21	
	740±18	700±17	654±18	

Fig. 6. Table showing the most representative core (upper row) and rim (lower row) analyses. Only highly concordant data accounting for clearly different crystallization ages (Ma) are included.

Eguiluz *et al.* 2000; Castiñeiras *et al.* 2010), and to a lesser extent by the Cambrian and Ordovician igneous activity that affected the continental platform (e.g. Montero *et al.* 2009; Díez Montes *et al.* 2010; Sánchez-García *et al.* 2010). However, the continental platform was subjected to contemporaneous, protracted extension and high subsidence rates (von Raumer & Stampfli 2008), so that the sources of Palaeozoic detritus were quickly buried under a sedimentary cover. As a result, the detritus that filled the basin that the Schistose Domain represents would have come mostly from inner parts of the continent. Conversely, the most distal part of the margin (e.g. basal units of the allochthonous complexes) would have been fed by synchronous tectonomagmatic arc activity.

The detrital zircon age spectra of the Schistose Domain and those of the basal units of the allochthonous complexes are strikingly similar (Fig. 5). Despite the Cambrian input of the youngest series of the basal units, the main populations and their respective percentages indicate that the palaeogeographical realms they represent were located next to the same continental exposures. These sources resemble those of the autochthonous sequences (Fernández-Suárez *et al.* 2000, 2002; Gutiérrez-Alonso *et al.* 2003; Martínez Catalán *et al.* 2004), so the two lower terranes of the allochthonous pile of NW Iberia would have shared a comparable palaeogeographical position during the Early Palaeozoic. As a consequence, none of the terranes located under the ophiolitic units should be considered as exotic.

The Neoproterozoic, Palaeoproterozoic and Archaean ages of the Schistose Domain indicate a West African Craton provenance (Nance & Murphy 1994). However, the middle and early Neoproterozoic signature (750–950 Ma; Cryogenian and Tonian), which is absent in this craton (Ennih & Liégeois 2008), has been recently proposed as a distinctive sediment provenance tracer for a mobile belt at its eastern boundary (Díez Fernández *et al.* 2010), the so-called Hoggar megasuture (Caby 2003). The Mesoproterozoic input present in the sequences of NW Iberia also occurs in this major tectonic zone (Stern *et al.* 1994; Henry *et al.* 2009), and both middle and early Neoproterozoic (Cryogenian and Tonian) and late Mesoproterozoic (Stenian) ages spanning 750–1200 Ma exist in the Cambrian sedimentary cover of Morocco, north of the West African

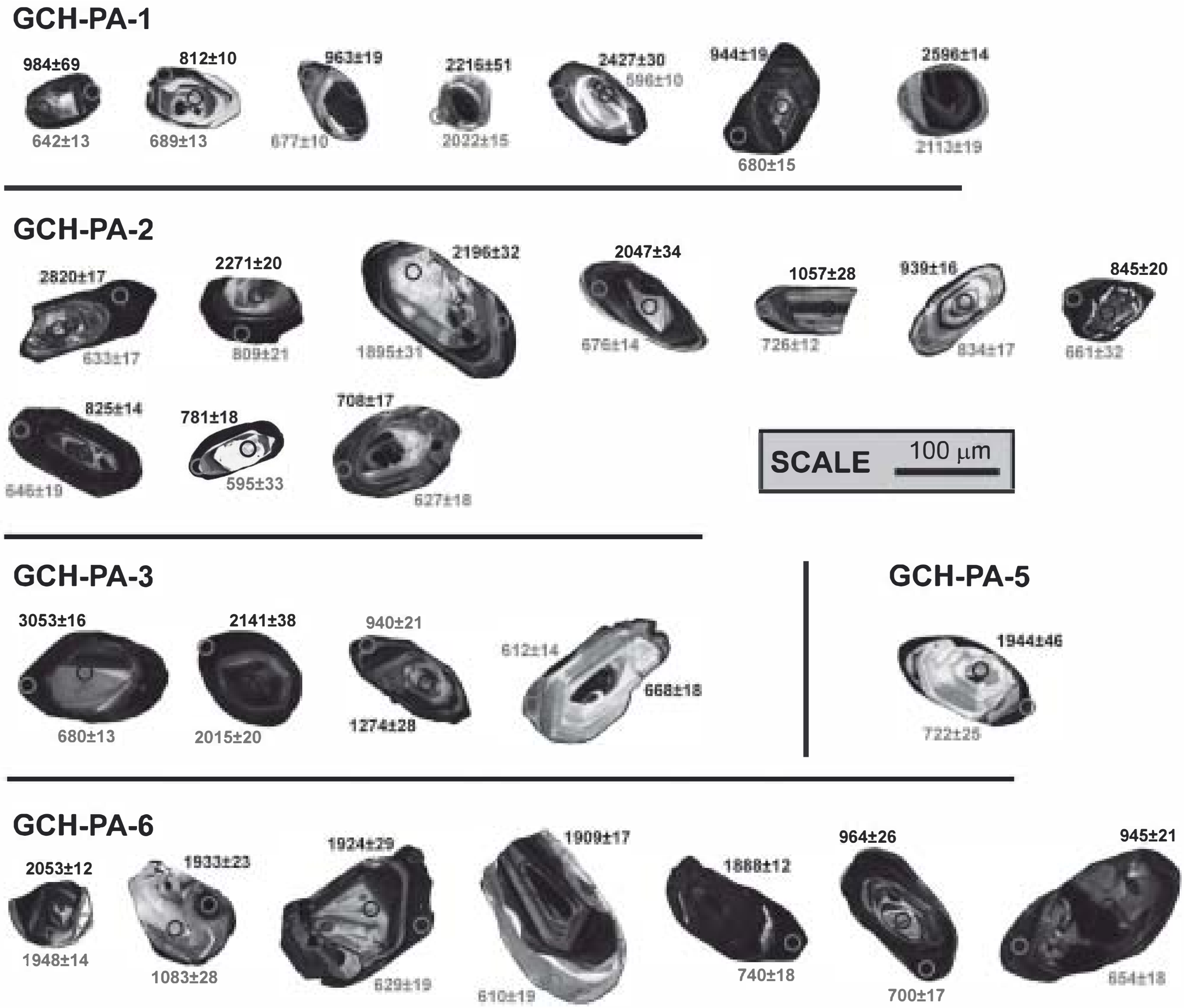

Fig. 7. Cathodoluminescence images of zircon grains showing core–rim internal structure, with indication of respective LA-ICP-MS U–Pb ages (black, core; grey, rim).

Craton (Avigad *et al.* 2012). On the other hand, the continental terranes forming part of the Variscan pile show a consistent decrease in their content of 750–1200 Ma zircons upward, from up to 38% in the autochthon to 14% in the Schistose Domain, 7% in the basal units, and 0% in the uppermost allochthon (Fernández-Suárez *et al.* 2002, 2003; Martínez Catalán *et al.* 2004; Díaz García *et al.* 2010; Díez Fernández *et al.* 2010). For this location along the northern margin of Gondwana, such a trend may indicate relative proximity to the Hoggar suture, with the NW Iberian terranes richer in 750–1200 Ma zircons having a more eastern derivation (Fig. 8). This palaeogeographical model is in agreement with recent data on model ages from whole-rock Nd (on meta-igneous Lower Ordovician rocks, Bea *et al.* 2010) and zircon Hf isotopes (granulitic rocks from central Spain, Villaseca *et al.* 2011), reinforcing a central African position of the innermost series of the autochthonous sequences of the Iberian Massif (the Central Iberian Zone) during late Neoproterozoic and Early Palaeozoic times.

For the uppermost allochthon of NW Iberia, the detrital sources suggest a different, yet Gondwanan provenance (Fig. 8), as pointed out by Fernández-Suárez *et al.* (2003). Its original position would have been to the west (present-day coordinates) of that of the basal units and the parautochthonous Schistose Domain, in front of the West African Craton.

The core and rim analyses also support the proposed palaeoposition of the Schistose Domain. For instance, the sequence of events recorded in some grains (Tonian cores and Cryogenian–Ediacaran rims) matches fairly well the tectonomagmatic evolution of some terranes involved in the Hoggar megasuture (e.g. the Iskel terrane; Caby 2003; Liégeois *et al.* 2003). Either the continuation of these terranes to the north, or reworked material coming from their dismantlement in the Gondwana interior, may have supplied reworked early Neoproterozoic zircons to the Gondwana periphery. Moreover, some grains suggest that Stenian rocks could have been involved in active zones at 750–900 Ma. There is no clear Stenian activity reported in the core of Gondwana so far, particularly in central and West Africa. However, its fingerprint (and even that of possible Ectasian and Calymmian events) can be vaguely followed in some ophiolitic units located in the peri-Gondwanan realms

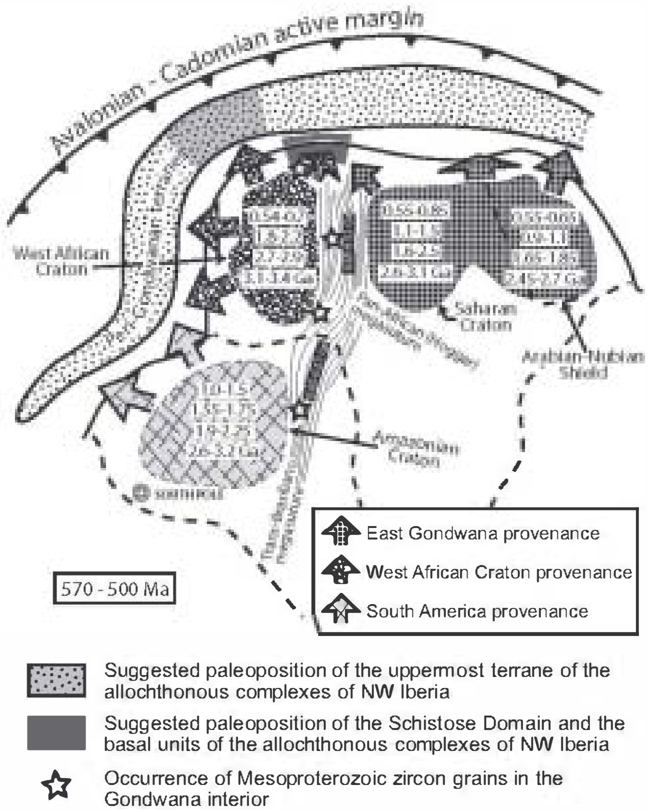

Fig. 8. Simplified palaeogeography of Gondwana and related major peri-Gondwanan terranes at 570–500 Ma (modified from Nance *et al.* 2002, Linnemann *et al.* 2007, and Cordani *et al.* 2009) showing the palaeoposition of the Schistose Domain, the basal allochthonous units, and the uppermost terrane of the allochthonous complexes of NW Iberia (after Díez Fernández *et al.* 2010). Numbers in the cratonic areas summarize their main age spectra for provenance constraints. The sites within the Gondwana interior containing Mesoproterozoic grains (stars) should be noted.

(Sánchez Martínez *et al.* 2011), in many terranes representing the margin of Gondwana, such as the NW Iberian terranes described in this paper (e.g. Murphy *et al.* 2008), and in the Cambrian sedimentary cover of Morocco (Avigad *et al.* 2012), the Tuareg Shield (Henry *et al.* 2009; Linnemann *et al.* 2011), and the Gulf of Guinea (Voltaian basin; Kalsbeek *et al.* 2008), where the Stenian event can be tentatively connected to the Mesoproterozoic Amazonian geodynamics through the Trans-Brasiliano megasuture (e.g. Cordani *et al.* 2009). These data provide evidence of a scarce, fragmentary Mesoproterozoic evolution along the intra- and peri-Gondwanan borders of the African cratons that was strongly overprinted by the Pan-African cycle.

Conclusions

The analysed series of the lower allochthon of NW Iberia have a latest Neoproterozoic maximum depositional age (*c.* 560 Ma) and were deposited at the northern boundary of the West African Craton, probably in front of, or just west of the northern prolongation of the Hoggar megasuture. The allochthonous terranes involved in the Variscan collision and located in the footwall of the suture zone (ophiolitic units) in NW Iberia should not be considered as exotic relative to the autochthonous sedimentary sequences deposited along the Gondwana margin, although they have undergone important thrust displacements. Some of the Mesoproterozoic detrital zircons are considered to have been derived from the African interior, and should be taken into account for palaeogeographical reconstructions of the Gondwanan periphery.

Our study not only provides several azoic series of northern Gondwana with new age constraints, but also contributes to a better understanding of Variscan tectonics by documenting a drop in Early Neoproterozoic and Mesoproterozoic zircon content toward the upper parts of the Variscan nappes. This relationship may help to ascertain the relative palaeoposition of other far-travelled terranes exposed in Europe, as well as to unravel exotic elements across the Gondwanan platform.

This study has been funded by research projects CGL2007-65338-C02-01 and -02/BTE of the Dirección General de Programas y Transferencia del Conocimiento (Spanish Ministry of Science and Innovation), co-financed by the European Funds of Regional Development (FEDER). This paper is a contribution to IGCP 497. B. Murphy and C. Villaseca are gratefully acknowledged for their careful revision of the paper and suggestions, and M. Whitehouse for the editorial work.

References

Abati, J., Dunning, G.R., Arenas, R., Díaz García, F., González Cuadra, P., Martínez Catalán, J.R. & Andonaegui, P. 1999. Early Ordovician orogenic event in Galicia (NW Spain): evidence from U–Pb ages in the uppermost unit of the Ordenes Complex. *Earth and Planetary Science Letters*, **165**, 213–228.

Abati, J., Gerdes, A., Fernández-Suárez, J., Arenas, R., Whitehouse, M.J. & Díez Fernández, R. 2010. Magmatism and early-Variscan continental subduction in the northern Gondwana margin recorded in zircons from the basal units of Galicia, NW Spain. *Geological Society of America Bulletin*, **122**, 219–235.

Ancochea, E., Arenas, R., Brandle, J.L., Peinado, M. & Sagredo, J. 1988. Caracterización de las rocas metavolcánicas silúricas del NO del Macizo Ibérico. *Geociencias, Aveiro*, **3**, 23–34.

Arenas, R. 1988. Evolución petrológica y geoquímica de la unidad alóctona inferior del complejo metamórfico básico-ultrabásico de Cabo Ortegal (Unidad de Moeche) y del Silúrico parautóctono, Cadena Hercínica Ibérica (NW de España). *Corpus Geologicum Gallaecia*, **4**, 1–543.

Arenas, R., Gil Ibarguchi, J.I., *et al.* 1986. Tectonostratigraphic units in the complexes with mafic and related rocks of the NW of the Iberian Massif. *Hercynica*, **2**, 87–110.

Arenas, R., Rubio Pascual, F.J., Díaz García, F. & Martínez Catalán, J.R. 1995. High-pressure micro-inclusions and development of an inverted metamorphic gradient in the Santiago schists (Ordenes Complex, NW Iberian Massif, Spain)—evidence of subduction and syncollisional decompression. *Journal of Metamorphic Geology*, **13**, 141–164.

Arenas, R., Martínez Catalán, J.R., Sánchez Martínez, S., Fernández-Suárez, J., Andonaegui, P., Pearce, J.A. & Corfú, F. 2007. The Vila de Cruces ophiolite: a remnant of the early Rheic Ocean in the Variscan suture of Galicia (northwest Iberian Massif). *Journal of Geology*, **115**, 129–148.

Arenas, R., Sánchez Martínez, S., Castiñeiras, P., Jeffries, T.E., Díez Fernández, R. & Andonaegui, P. 2009. The basal tectonic melange of the Cabo Ortegal Complex (NW Iberian Massif): a key unit in the suture of Pangea. *Journal of Iberian Geology*, **35**, 85–125.

Avigad, D., Gerdes, A., Morag, N. & Bechstädt, T. 2012. Coupled U–Pb-Hf of detrital zircons of Cambrian sandstones from Morocco and Sardinia: implications for provenance and Precambrian crustal evolution of North Africa. *Gondwana Research*, **21**, 690–703.

Barrera, J.L., Farias, P., *et al.* 1989. *Mapa y memoria de la Hoja n° 17-27 (Orense-Verín) del Mapa Geológico de España, Escala 1/200.000*. Instituto Geológico y Minero de España, Madrid.

Bea, F., Montero, P., Talavera, C., Abu Anbar, M., Scarrow, J.H., Molina, J.F. & Moreno, J.A. 2010. The palaeogeographic position of Central Iberia in Gondwana during the Ordovician: evidence from zircon chronology and Nd isotopes. *TerraNova*, **22**, 341–346.

Braid, J.A., Murphy, J.B., Quesada, C. & Mortensen, J. 2011. Tectonic escape of a crustal fragment during the closure of the Rheic Ocean: U–Pb detrital zircon data from the Late Palaeozoic Pulo do Lobo and South Portuguese zones, southern Iberia. *Journal of the Geological Society, London*, **168**, 383–392.

Caby, R. 2003. Terrane assembly and geodynamic evolution of central–western Hoggar: a synthesis. *Journal of African Earth Sciences*, **37**, 133–159.

Castiñeiras, P., Díaz García, F. & Gómez Barreiro, J. 2010. REE-assisted U–Pb zircon age (SHRIMP) of an anatectic granodiorite: constraints on the evolution of the A Silva granodiorite, Iberian allochthonous complexes. *Lithos*, **116**, 153–166.

Cordani, U.G., Teixeira, W., D'Agrella, M.S. & Trindade, R.I. 2009. The position of the Amazonian craton in supercontinents. *Gondwana Research*, **15**, 396–407.

Chang, Z., Vervoort, J.D., McClelland, W.C. & Knaack, C. 2006. U–Pb dating of zircon by LA-ICP-MS. *Geochemistry, Geophysics, Geosystems*, **7**, Q05009, doi: 10.1029/2005gc001100.

Dias Da Silva, I. & González Clavijo, E. 2010. New data on tectonometamorphic evolution of the Peri-Trasmontano domain (Schistose Domain) in Northeastern Portugal. *Boletín Geológico y Minero*, **121**, 45–56.

Dias Da Silva, I., Valverde-Vaquero, P., González Clavijo, E., Díez Montes, A. & Martínez Catalán, J.R. 2012. Structural and stratigraphical significance of U–Pb ages from the Saldanha and Mora volcanic complexes (NE Portugal, Iberian Variscides). *In*: *Length Scales, Times Scales and Relative Contribution of Variscan Orogenic Events to Formation of European Crust.* Géologie de la France/BRGM, France, **1**, 105–106.

Díaz García, F., Arenas, R., Martínez Catalán, J.R., del Tanago, J.G. & Dunning, G.R. 1999. Tectonic evolution of the Careon ophiolite (northwest Spain). A remnant of oceanic lithosphere in the Variscan belt. *Journal of Geology*, **107**, 587–605.

Díaz García, F., Sánchez Martínez, S., Castiñeiras, P., Fuenlabrada, J.M. & Arenas, R. 2010. A peri-Gondwanan arc in NW Iberia II: assessment of the intra-arc tectonothermal evolution through U–Pb SHRIMP dating of mafic dykes. *Gondwana Research*, **17**, 352–362.

Díez Fernández, R. & Martínez Catalán, J.R. 2009. 3D analysis of an Ordovician igneous ensemble: a complex magmatic structure hidden in a polydeformed allochthonous Variscan unit. *Journal of Structural Geology*, **31**, 222–236.

Díez Fernández, R., Martínez Catalán, J.R., Gerdes, A., Abati, J., Arenas, R. & Fernández-Suárez, J. 2010. U–Pb ages of detrital zircons from the basal allochthonous units of NW Iberia: provenance and paleoposition on the northern margin of Gondwana during the Neoproterozoic and Paleozoic. *Gondwana Research*, **18**, 385–399.

Díez Fernández, R., Castiñeiras, P. & Gómez Barreiro, J. 2012*a*. Age constraints on lower Paleozoic convection system: magmatic events in the NW Iberian Gondwana margin. *Gondwana Research*, **21**, 1066–1079.

Díez Fernández, R., Martínez Catalán, J.R., Gómez Barreiro, J. & Arenas, R. 2012*b*. Extensional flow during gravitational collapse: a tool for setting plate convergence (Padrón migmatitic dome, Variscan belt, NW Iberia). *Journal of Geology*, **120**, 83–103.

Díez Montes, A., Martínez Catalán, J.R. & Bellido Mulas, F. 2010. Role of the Ollo de Sapo massive felsic volcanism of NW Iberia in the early Ordovician dynamics of northern Gondwana. *Gondwana Research*, **17**, 363–376.

Drost, K., Gerdes, A., Jeffries, T., Linnemann, U. & Storey, C. 2011. Provenance of Neoproterozoic and early Paleozoic siliciclastic rocks of the Teplá–Barrandian unit (Bohemian Massif): evidence from U–Pb detrital zircon ages. *Gondwana Research*, **19**, 213–231.

Eguiluz, L., Gil Ibarguchi, J.I., Abalos, B. & Apraiz, A. 2000. Superposed Hercynian and Cadomian orogenic cycles in the Ossa–Morena zone and related areas of the Iberian Massif. *Geological Society of America Bulletin*, **112**, 1398–1413.

Ennih, N. & Liégeois, J.P. 2008. The boundaries of the West African craton, with special reference to the basement of the Moroccan metacratonic Anti-Atlas belt. *In*: Ennih, N. & Liégeois, J.P. (eds) *The Boundaries of the West African Craton*. Geological Society, London, Special Publication, **297**, 1–17.

Farias, P. & Marcos, A. 2004. Dominio Esquistoso de Galicia–Tras-os-Montes. *In*: Vera, J.A. (ed.) *Geología de España*. SGE-IGME, Madrid, 135–138.

Farias, P., Gallastegui, G., et al. 1987. Aportaciones al conocimiento de la litoestratigrafía y estructura de Galicia Central. *Memorias da Faculdade de Ciencias, Universidade do Porto*, **1**, 411–431.

Fernández-Suárez, J., Gutiérrez-Alonso, G., Jenner, G.A. & Tubrett, M.N. 2000. New ideas on the Proterozoic–Early Palaeozoic evolution of NW Iberia: insights from U–Pb detrital zircon ages. *Precambrian Research*, **102**, 185–206.

Fernández-Suárez, J., Gutiérrez-Alonso, G., Cox, R. & Jenner, G.A. 2002. Assembly of the Armorica microplate: a strike-slip terrane delivery? Evidence from U–Pb ages of detrital zircons. *Journal of Geology*, **110**, 619–626.

Fernández-Suárez, J., Díaz García, F., Jeffries, T.E., Arenas, R. & Abati, J. 2003. Constraints on the provenance of the uppermost allochthonous terrane of the NW Iberian Massif: inferences from detrital zircon U–Pb ages. *Terra Nova*, **15**, 138–144.

Frei, D. & Gerdes, A. 2009. Precise and accurate in situ U–Pb dating of zircon with high sample throughput by automated LA-SF-ICP-MS. *Chemical Geology*, **261**, 261–270.

Fuenlabrada, J.M., Arenas, R., Sánchez Martínez, S., Díaz García, F. & Castiñeiras, P. 2010. A peri-Gondwanan arc in NW Iberia: I: isotopic and geochemical constraints on the origin of the arc—a sedimentary approach. *Gondwana Research*, **17**, 338–351.

Gallastegui, G., Martín Parra, L.M., de Pablo Maciá, J.G. & Rodríguez-Fernández, L.R. 1987. Las metavulcanitas del Dominio Esquistoso de Galicia–Tras-os-Montes: petrografía, geoquímica y ambiente geotectónico (Galicia, NO de España). *Cuadernos do Laboratorio Xeolóxico de Laxe*, **12**, 127–139.

Gerdes, A. & Zeh, A. 2006. Combined U–Pb and Hf isotope LA-(MC-)ICP-MS analyses of detrital zircons: comparison with SHRIMP and new constraints for the provenance and age of an Armorican metasediment in Central Germany. *Earth and Planetary Science Letters*, **249**, 47–61.

Gerdes, A. & Zeh, A. 2009. Zircon formation versus zircon alteration—new insights from combined U–Pb and Lu–Hf *in-situ* LA-ICP-MS analyses, and consequences for the interpretation of Archean zircon from the Central Zone of the Limpopo Belt. *Chemical Geology*, **261**, 230–243.

Gómez Barreiro, J., Martínez Catalán, J.R., Arenas, R., Castiñeiras, P., Abati, J., Díaz García, F. & Wijbrans, J.R. 2007. Tectonic evolution of the upper allochthon of the Órdenes Complex (northwestern Iberian Massif): structural constraints to a polyorogenic peri-Gondwanan terrane. *In*: Linnemann, U., Nance, R.D., Kraft, P. & Zulauf, G. (eds) *The Evolution of the Rheic Ocean: From Avalonian–Cadomian Active Margin to Alleghenian–Variscan Collision*. Geological Society of America, Special Papers, **423**, 315–332.

Gómez Barreiro, J., Martínez Catalán, J.R., Díez Fernández, R., Arenas, R. & Díaz García, F. 2010. Upper crust reworking during gravitational collapse: the Bembibre–Pico Sacro detachment system (NW Iberia). *Journal of the Geological Society, London*, **167**, 769–784.

González Clavijo, E. & Martínez Catalán, J.R. 2002. Stratigraphic record of preorogenic to synorogenic sedimentation and tectonic evolution of imbricate units in the Alcañices synform (northwestern Iberian Massif). *In*: Martínez Catalán, J.R., Hatcher, R.D., Arenas, R. & Díaz García, F. (eds) *Variscan–Appalachian Dynamics: The Building of the Late Paleozoic Basement*. Geological Society of America, Special Papers, 17–35.

Gutiérrez-Alonso, G., Fernández-Suárez, J., Jeffries, T.E., Jenner, G.A., Tubrett, M.N., Cox, R. & Jackson, S.E. 2003. Terrane accretion and dispersal in the northern Gondwana margin. An early Paleozoic analogue of a long-lived active margin. *Tectonophysics*, **365**, 221–232.

Gutiérrez-Marco, J.C., Sarmiento, G.N., Robardet, M., Rábano, I. & Vanek, J. 2001. Upper Silurian fossils of Bohemian type from NW Spain and their palaeogeographical interest. *Journal of the Czech Geological Society*, **46**, 247–258.

Henry, B., Liégeois, J.P., et al. 2009. Repeated granitoid intrusions during the Neoproterozoic along the western boundary of the Saharan metacraton, Eastern Hoggar, Tuareg shield, Algeria: an AMS and U–Pb zircon age study. *Tectonophysics*, **474**, 417–434.

Hoskin, P.W.O. 2000. Patterns of chaos: fractal statistics and the oscillatory chemistry of zircon. *Geochimica et Cosmochimica Acta*, **64**, 1905–1923.

Iglesias, M. & Robardet, M. 1980. El Silúrico de Galicia Media (Central), su importancia en la paleogeografía varisca. *Cuadernos do Laboratorio Xeolóxico de Laxe*, **1**, 99–115.

Jackson, S.E., Pearson, N.J., Griffin, W.L. & Belousova, E.A. 2004. The application of laser ablation-inductively coupled plasma-mass spectrometry to *in situ* U–Pb zircon geochronology. *Chemical Geology*, **211**, 47–69.

Janousek, V., Gerdes, A., Vrana, S., Finger, F., Erban, V., Friedl, G. & Braithwaite, C.J.R. 2006. Low-pressure granulites of the Lisov Massif, Southern Bohemia: Visean metamorphism of Late Devonian plutonic arc rocks. *Journal of Petrology*, **47**, 705–744.

Kalsbeek, F., Frei, D. & Affaton, P. 2008. Constraints on provenance, stratigraphic correlation and structural context of the Volta basin, Ghana, from detrital zircon geochronology: an Amazonian connection? *Sedimentary Geology*, **212**, 86–95.

Liégeois, J.P., Latouche, L., Boughrara, M., Navez, J. & Guiraud, M. 2003. The LATEA metacraton (Central Hoggar, Tuareg shield, Algeria): behaviour of an old passive margin during the Pan-African orogeny. *Journal of African Earth Sciences*, **37**, 161–190.

Linnemann, U., Gerdes, A., Drost, K. & Buschmann, B. 2007. The continuum between Cadomian orogenesis and opening of the Rheic Ocean: constraints from LA-ICP-MS U–Pb zircon dating and analysis of plate-tectonic setting (Saxo-Thuringian zone, northeastern Bohemian Massif, Germany). *In*: Linnemann, U., Nance, R.D., Kraft, P. & Zulauf, G. (eds) *The Evolution of the Rheic Ocean: From Avalonian–Cadomian Active Margin to Alleghenian–Variscan Collision*. Geological Society of America, Special Papers, **423**, 61–96.

Linnemann, U., Ouzegane, K., Drareni, A., Hofmann, M., Becker, S., Gartner, A. & Sagawe, A. 2011. Sands of West Gondwana: an archive of secular magmatism and plate interactions—a case study from the Cambro-Ordovician section of the Tassili Ouan Ahaggar (Algerian Sahara) using U–Pb LA-ICP-MS detrital zircon ages. *Lithos*, **123**, 188–203.

Ludwig, K.R. 2003. *User's Manual for Isoplot 3.00: A Geochronological Toolkit for Microsoft Excel.* Berkeley Geochronology Center, Special Publication, 4.

Marcos, A. & Farias, P. 1999. La estructura de las láminas inferiores del Complejo de Cabo Ortegal y su autóctono relativo (Galicia, NW de España). *Trabajos de Geología*, **21**, 201–220.

Marcos, A. & Llana-Fúnez, S. 2002. Estratigrafía y estructura de la lámina tectónica del Para-autóctono y de su autóctono en el área de Chantada (Galicia, NO de España). *Trabajos de Geología*, **23**, 53–72.

Marquínez García, J.L. 1984. *La geología del área esquistosa de Galicia Central (Cordillera Herciniana, NW de España). Memorias del Instituto Geológico y Minero de España*, **100**.

Martínez Catalán, J.R. 1990. A non-cylindrical model for the northwest Iberian allochthonous terranes and their equivalents in the Hercynian belt of Western Europe. *Tectonophysics*, **179**, 253–272.

Martínez Catalán, J.R., Arenas, R., Díaz García, F., Rubio Pascual, F.J., Abati, J. & Marquínez García, J. 1996. Variscan exhumation of a subducted Paleozoic continental margin: the basal units of the Ordenes Complex, Galicia, NW Spain. *Tectonics*, **15**, 106–121.

Martínez Catalán, J.R., Arenas, R., Díaz García, F. & Abati, J. 1997. Variscan accretionary complex of northwest Iberia: terrane correlation and succession of tectonothermal events. *Geology*, **25**, 1103–1106.

Martínez Catalán, J.R., Díaz García, F., et al. 2002. Thrust and detachment systems in the Ordenes complex (northwestern Spain): implications for the Variscan–Appalachian geodynamics. *In*: Martínez Catalán, J.R., Hatcher, R.D., Arenas, R. & Díaz García, F. (eds) *Variscan–Appalachian Dynamics: The Building of the Late Paleozoic Basement.* Geological Society of America, Special Papers, 163–182.

Martínez Catalán, J.R., Fernández-Suárez, J., Jenner, G.A., Belousova, E. & Díez Montes, A. 2004. Provenance constraints from detrital zircon U–Pb ages in the NW Iberian Massif: implications for Palaeozoic plate configuration and Variscan evolution. *Journal of the Geological Society, London*, **161**, 463–476.

Martínez Catalán, J.R., Arenas, R., et al. 2009. A rootless suture and the loss of the roots of a mountain chain: the Variscan belt of NW Iberia. *Comptes Rendus Géoscience*, **341**, 114–126.

Montero, P., Talavera, C., Bea, F., Lodeiro, F.G. & Whitehouse, M.J. 2009. Zircon geochronology of the Ollo de Sapo Formation and the age of the Cambro-Ordovician rifting in Iberia. *Journal of Geology*, **117**, 174–191.

Murphy, J.B., Gutiérrez-Alonso, G., Fernández-Suárez, J. & Braid, J.A. 2008. Probing crustal and mantle lithosphere origin through Ordovician volcanic rocks along the Iberian passive margin of Gondwana. *Tectonophysics*, **461**, 166–180.

Nance, R.D. & Murphy, J.B. 1994. Contrasting basement isotopic signatures and the palinspastic restoration of peripheral orogens: example from the Neoproterozoic Avalonian–Cadomian belt. *Geology*, **22**, 617–620.

Nance, R.D., Murphy, J.B. & Keppie, J.D. 2002. A Cordilleran model for the evolution of Avalonia. *Tectonophysics*, **352**, 11–31.

Pereira, Z., Meireles, C. & Pereira, E. 1999. Upper Devonian palynomorphs of the NE sector of Trás-os-Montes (Central Iberian Zone). *In*: Gámez Vintaned, J.A., Eguíluz, L. & Palacios, T. (eds) *XV Reunión de Geología del Oeste Peninsular—International Meeting on Cadomian Orogens, Badajoz, Spain, Extended Abstracts.* Diputación de Badajoz, Badajoz, 201–206.

Piçarra, J.M., Gutiérrez-Marco, J.C., Sá, A.A., Meireles, C. & González Clavijo, E. 2006. Silurian graptolite biostratigraphy of the Galicia–Trás-os-Montes Zone (Spain and Portugal). *GFF*, **128**, 185–188.

Pin, C., Paquette, J.L., Abalos, B., Santos, F.J. & Gil Ibarguchi, J.I. 2006. Composite origin of an early Variscan transported suture: ophiolitic units of the Morais Nappe Complex (north Portugal). *Tectonics*, **25**, TC5001, doi: 10.1029/2006tc001971.

Ribeiro, A., Pereira, E. & Dias, R. 1990. Structure in the northwest of the Iberian Peninsula. *In*: Dallmeyer, R.D. & Martínez García, E. (eds) *Pre-Mesozoic Geology of Iberia.* Springer, Berlin, 220–236.

Rodrigues, J., Pereira, E. & Ribeiro, A. 2006. Estrutura interna do Complexo de Mantos Parautóctones, sector de Murça–Mirandela (NE de Portugal). *In*: Dias, R., Araújo, A., Terrinha, P. & Kullberg, C. (eds) *Geologia de Portugal no contexto da Ibéria.* Universidade de Évora, Évora, 63–84.

Rodríguez, R., Marcos, A. & Farias, P. 2004. Palynological data on the age of the meta-sediments of the 'Schistose Domain' in the Cabo Ortegal área (Galicia–Trás-os-Montes Zone). *Neues Jahrbuch für Geologie und Paläontologie*, **4**, 214–232.

Sánchez-García, T., Bellido, F., Pereira, M.F., Chichorro, M., Quesada, C., Pin, C. & Silva, J.B. 2010. Rift-related volcanism predating the birth of the Rheic Ocean (Ossa–Morena zone, SW Iberia). *Gondwana Research*, **17**, 392–407.

Sánchez Martínez, S., Arenas, R., Díaz García, F., Martínez Catalán, J.R., Gómez Barreiro, J. & Pearce, J.A. 2007. Careon ophiolite, NW Spain: Suprasubduction zone setting for the youngest Rheic Ocean floor. *Geology*, **35**, 53–56.

Sánchez Martínez, S., Arenas, R., Gerdes, A., Castiñeiras, P., Gómez Barreiro, J., Potrel, A. & Fernández-Suárez, J. 2011. Isotope geochemistry and revised geochronology of the Purrido Ophiolite (Cabo Ortegal Complex, NW Iberian Massif): Devonian magmatism with mixed sources and involved Mesoproterozoic basement. *Journal of the Geological Society, London*, **168**, 733–750.

Sarmiento, G.N., Piçarra, J.M., Rebelo, J.A., Robardet, M., Gutiérrez-Marco, J.C., Storch, P. & Rábano, I. 1999. Le silurien du synclinorium de Moncorvo (NE du Portugal): Biostratigraphie et importance paléogéographique. *Geobios*, **32**, 749–767.

Sircombe, K.N. 2004. AgeDisplay: an EXCEL workbook to evaluate and display univariate geochronological data using binned frequency histograms and probability density distributions. *Computers and Geosciences*, **30**, 21–31.

Sláma, J., Košler, J., et al. 2008. Plešovice zircon—a new natural reference material for U–Pb and Hf isotopic microanalysis. *Chemical Geology*, **249**, 1–35.

Stacey, J.S. & Kramers, J.D. 1975. Approximation of terrestrial lead isotope evolution by a 2-stage model. *Earth and Planetary Science Letters*, **26**, 207–221.

Stern, R., Kröner, A., Bender, R., Reischmann, T. & Dawoud, A. 1994. Precambrian basement around Wadi Halfa, Sudan: a new perspective on the evolution of the East Saharan Craton. *Geologische Rundschau*, **83**, 564–577.

Valverde-Vaquero, P., Marcos, A., Farias, P. & Gallastegui, G. 2005. U–Pb dating of Ordovician felsic volcanism in the Schistose Domain of the Galicia–Trás-os-Montes Zone near Cabo Ortegal (NW Spain). *Geologica Acta*, **3**, 27–37.

Villaseca, C., Belousova, E., Orejana, D., Castiñeiras, P. & Pérez-Soba, C. 2011. Presence of Palaeoproterozoic and Archean components in the granulite-facies rocks of central Iberia: the Hf isotopic evidence. *Precambrian Research*, **187**, 143–154.

Von Raumer, J.F. & Stampfli, G.M. 2008. The birth of the Rheic Ocean—early Palaeozoic subsidence patterns and subsequent tectonic plate scenarios. *Tectonophysics*, **461**, 9–20.

Zhu, W., Zheng, B., et al. 2011. Neoproterozoic tectonic evolution of the Precambrian Aksu blueschist terrane, northwestern Tarim, China: insights from LA-ICP-MS zircon U–Pb ages and geochemical data. *Precambrian Research*, **185**, 215–230.